

Dual Flexible Prescribed Performance Control of Input Saturated High-Order Nonlinear Systems

Yangang Yao¹, Xu Liang, Yu Kang², Yunbo Zhao³, *Senior Member, IEEE*, Jieqing Tan⁴, and Lichuan Gu⁵

Abstract—This article first presents a dual flexible prescribed performance control (DFPPC) approach of input saturated high-order nonlinear systems (IS-HONSSs). Compared to the existing PPC approaches of IS-HONSSs, under which the performance constraint boundaries (PCBs) are usually fixed and bounded, resulting in a restriction of the initial error in the algorithm implementation; in addition, the coupling relationship between performance constraints and input saturation is usually ignored, resulting in the methods are very fragile when input saturation occurs. By designing the novel tensile model-based PCBs that depend on output and input constraints, the proposed DFPPC method provides sufficient resilience for both the initial conditions and the input saturation, so that the proposed DFPPC method can not only be suitable for multiple types of initial errors by adjusting the parameters, including $e_1(0) \in (\underline{\mathcal{B}}(0), \bar{\mathcal{B}}(0))$, $e_1(0) \in (-\infty, \bar{\mathcal{B}}(0))$, $e_1(0) \in (\underline{\mathcal{B}}(0), +\infty)$ and $e_1(0) \in (-\infty, \infty)$, where $\underline{\mathcal{B}}(0)$ and $\bar{\mathcal{B}}(0)$ denote the initial PCBs; but also can achieve a good balance between input saturation and performance constraints, i.e., when the control input reaches or exceeds the saturation threshold, the PCBs can adaptively extend to avoid the singularity, and when the control input returns to the saturation threshold range, the PCBs are then adaptively restored to the original PCBs. The results show that the proposed DFPPC algorithm guarantees semi-global boundedness for all closed-loop signals, while ensuring that the system output accurately tracks the desired signal, and it consistently maintains the tracking error

within the PCBs. The developed algorithm is illustrated by means of simulation instances.

Index Terms—Dual flexible prescribed performance control (DFPPC), high-order nonlinear systems, input saturation.

I. INTRODUCTION

IT IS widely acknowledged that most of actual systems commonly face diverse constraints. Broadly speaking, these constraints can be divided into two categories: one is related to the carrying capacity of the system, such as state/output/input constraints; and the other is the performance constraints related to overshooting, convergence time, and tracking accuracy. The violation of the above constraints may reduce the control performance, and even cause the system to lose control and instability. Over the past few decades, a great deal of control methods for state/output-constrained nonlinear systems have been presented, including the barrier function-based methods [1], [2], [3], [4], [5], mapping transformation-based methods [6], [7], [8], [9], [10], [11], and so on. In addition, to achieve better steady and transient-state performance, Bechlioulis and Rovithakis [12] innovatively proposed a PPC method, the core of which is to constrain the tracking error within the exponential-type performance constraint boundaries (PCBs). Subsequently, the PPC (Hereinafter referred to as standard PPC (SPPC)) approach was extended to nonlinear systems with different forms [13], [14], [15], [16]. It is worth noting that the upper and lower PCBs of the SPPC methods are strictly monotone, resulting in the convergence time and tracking accuracy of the system can not be accurately predicted in advance, so that the application of the SPPC method is somewhat limited.

The convergence time and tracking accuracy are widely regarded as two important indexes in practical control systems, and a plethora of approaches focus on the above issues have been proposed. For instance, the finite/fixed-time control schemes [17], [18], [19], [20], the prescribed tracking accuracy schemes [21], [22] were proposed. The schemes presented in [17], [18], [19], [20], and [21], however, have limitations in that the upper bound of the convergence time is contingent upon multiple control parameters or initial system states, and the method proposed in [22] ignores the convergence time, thus weakening their application in real control systems. Then, the prescribed-time control [23], [24], [25], [26], [27], [28] were proposed, under which the convergence time can be predetermined and remains unaffected by the initial state and other control parameters. Furthermore, in order to simultaneously preset the convergence time and tracking accuracy of

Received 27 October 2024; revised 14 December 2024; accepted 27 December 2024. Date of publication 23 January 2025; date of current version 7 March 2025. This work was supported in part by the Anhui Provincial Department of Education Research Project under Grant 2024AH040082, and in part by the National Natural Science Foundation of China under Grant 62103394, Grant 62173317, Grant 62033012, and Grant 61725304. This article was recommended by Associate Editor L. Celentano. (Corresponding authors: Yu Kang; Lichuan Gu.)

Yangang Yao and Lichuan Gu are with the School of Information and Artificial Intelligence, the Anhui Province Key Laboratory of Smart Agricultural Technology and Equipment, and the Key Laboratory of Agricultural Sensors, Ministry of Agriculture and Rural Affairs, Anhui Agricultural University, Hefei 230036, China (e-mail: ygyao@ustc.edu.cn; glc@ahau.edu.cn).

Xu Liang is with the School of Information and Artificial Intelligence, Anhui Agricultural University, Hefei 230036, China (e-mail: 23723181@stu.ahau.edu.cn).

Yu Kang is with the Department of Automation and the Anhui Province Key Laboratory of Intelligent Low-Carbon Information Technology and Equipment, University of Science and Technology of China, Hefei 230027 China, also with the Institute of Advanced Technology, University of Science and Technology of China, Hefei 230088, China, and also with the Institute of Artificial Intelligence, Hefei Comprehensive National Science Center, Hefei 230088, China (e-mail: kangduyu@ustc.edu.cn).

Yunbo Zhao is with the Department of Automation, University of Science and Technology of China, Hefei 230027, China (e-mail: yzbzhao@ustc.edu.cn).

Jieqing Tan is with School of Mathematics, Hefei University of Technology, Hefei 230601, China (e-mail: jieqingtan@hfut.edu.cn).

Color versions of one or more figures in this article are available at <https://doi.org/10.1109/TCYB.2024.3524242>.

Digital Object Identifier 10.1109/TCYB.2024.3524242

the system, some novel control approaches combining SPPC and finite/fixed/prescribed-time control were proposed [29], [30], [31], [32]. It is important to note that this combination will introduce the complexity of computational and control design. To this end, by constructing the novel segmented PCBs, Zhao et al. [33] first presented a prescribed-time PPC (PTPPC) algorithm, under which the steady-state accuracy and convergence time can be set in advance. The PTPPC method was subsequently expanded to encompass nonlinear systems with diverse structures [34], [35], [36], [37], [38], [39]. However, since the initial PCBs in both SPPC and PTPPC methods can only be bounded, there is an inherent limitation in the SPPC and PTPPC methods, i.e., when the reference signal or the initial state is changed, the user has to recheck if the original parameters still satisfies the new initial conditions, and the designed controller becomes unsuitable if this condition is not met. Even worse, in some actual control systems (such as missile interceptors), the initial tracking error may be entirely unknown or only the symbol of the tracking error is known. Obviously, under the circumstances, the SPPC and PTPPC methods will no longer apply. To this end, Zhao et al. [40] proposed a unified PPC (UPPC) approach, which is suitable for multiple types of initial errors by adjusting parameters. Afterwards, The UPPC method was extend to strict-feedback systems [41], nonlinear systems with unknown time-varying coefficients [42] and error constrained nonlinear systems [43]. Note that the approaches proposed in [40], [41], [42], and [43], however, were based on the assumption of disregarding input saturation, which is clearly incongruous with the actual control systems.

Input constraint (or input saturation) is a common phenomenon in real control systems [44], [45], [46]. In the past decades, the PPC for input saturated nonlinear system has received extensive attention, and some effective control algorithms have been proposed [47], [48], [49], the core of which lies in transforming saturated input into a manageable normal input through diverse transformations. To just name a list, two SPPC methods based on auxiliary systems dealing with input saturation were proposed in [47] and [48]. Shen et al. [49] presented a PTPPC approach for a 2-DOF helicopter subject to input saturation. The noteworthy aspect is that the aforementioned schemes address input saturation and performance constraints as independent entities, assuming their concurrent implementation. In fact, the two are interrelated and usually in opposition, i.e., when the input reaches the saturation threshold, the actual control input is replaced by the saturation threshold, which may cause the tracking error to approach or violate the PCBs, resulting in a singular problem. On the contrary, too strict performance constraints will result in input saturation. Recently, the flexible PPC (FPPC) methods were proposed in [50], [51], and [52], which establish the correlation between performance constraints and input saturation, enabling a tradeoff to be achieved between the two. Then, the idea was extended to switched systems [53], time-delay systems [54], MIMO systems [55], mechanical systems [56], and nonlinear systems with strong external disturbances [57]. However, the initial PCBs in the above methods are always bounded, and once the initial error is changed, the methods

may not be effective. In addition, the majority of the existing PPC approaches concentrate on general feedback systems, and are not suitable for HONSs. The above analysis inspires us to design a novel dual flexible prescribed performance control (DFPPC) method for input saturated high-order nonlinear systems (IS-HONSs), which not only can be adapted to multiple types of initial errors by adjusting the parameters, but also can achieve a good balance between performance constraints and input saturation.

In summary, this article primarily focus on DFPPC of IS-HONSs, which remains unresolved in prior research. The main contributions are summarized as follows.

- 1) Different from the SPPC approaches [12], [13], [14], [15], [16], PTPPC approaches [33], [34], [35], [36], [37], [38] for nonlinear systems without considering the input saturation, and the FPPC approaches [50], [51], [52], [53], [54], [55] for input saturated nonlinear systems, under which there is always a restriction of the initial error in the algorithm implementation, i.e., when the reference signal or the initial state is changed, the user has to recheck if the original parameters still satisfies the new initial conditions, and the designed controller becomes unsuitable if this condition is not met. By designing the novel dual flexible PCBs, the proposed method provides sufficient flexibility for initial error, so that the proposed method can be adapted to multiple types of initial conditions by adjusting the parameters (see Remark 3), which implies that the proposed DFPPC algorithm has stronger applicability than the SPPC approaches [12], [13], [14], [15], [16], PTPPC approaches [33], [34], [35], [36], [37], [38] and FPPC approaches [50], [51], [52], [53], [54], [55].
- 2) Compared to the existing UPPC approaches [40], [41], [42], [43] for nonlinear systems without considering the input saturation, and the PPC approaches of input saturated nonlinear systems [47], [48], [49], which either ignore input saturation or ignore the interaction between performance constraints and input saturation, resulting in the methods are very fragile when input saturation occurs. In this article, an auxiliary system is introduced to establish the relationship between input saturation and performance constraints, and the novel tensile model-based PCBs that depend on output and input constraints is designed, so that the fragility in existing PPC methods is removed, i.e., when the control input reaches the maximum allowed threshold, the PCBs can adaptively extend to avoid the singularity, and when the control input returns to the saturation threshold range, the PCBs are then adaptively restored to the original PCBs.

II. PROBLEM FORMULATION AND IMPORTANT LEMMAS

A. Problem Formulation

Give the following IS-HONSs:

$$\begin{cases} \dot{x}_i = f_i(\bar{x}_i) + x_{i+1}^{p_i}, i = 1, 2, \dots, n-1 \\ \dot{x}_n = f_n(\bar{x}_n) + u^{p_n}(v) \\ y = x_1 \end{cases} \quad (1)$$

where $\bar{x}_i = [x_1, \dots, x_i]^T \in R^i$ stands for the system state vector, $y \in R$ and $u(v) \in R$ stand for the system output and input, respectively, $v \in R$ serves as the designed controller. $f_i(\cdot) \in R$ stands for an uncertain continuous nonlinear function, $p_i \in R_{odd}^{\geq 1} = \{p \geq 1 | p = q_1/q_2\}$, $q_j \in R^+$ ($j = 1, 2$) with $i = 1, 2, \dots, n$, and

$$u(v) = \begin{cases} v, & |v| \leq u_d \\ \text{sgn}(v)u_d, & |v| > u_d \end{cases} \quad (2)$$

where u_d stands for the maximum allowable threshold for the control input.

Employ the following estimation to address the acute angles of $u(v)$:

$$u(v) = g_1(v) + g_2(v) \quad (3)$$

with $g_2(v) = u(v) - g_1(v)$, $g_1(v) = u_d \tanh(v/u_d)$, and $|g_2(v)| \leq u_d(1 - \tanh(1)) = \bar{g}$.

On the basis of the mean value theorem, for $\forall v_0 \in R$, we have

$$g'_1(v_1) = \frac{g_1(v) - g_1(v_0)}{v - v_0} \quad (4)$$

where $v_1 = v_0 + \lambda(v - v_0)$ with $\lambda \in (0, 1)$. Let $g_0 = g'_1(v_1)$, it can be known from the expression of $g_1(v)$ that $0 < \underline{g} \leq g_0^{p_n} < 1$, where \underline{g} denotes an unknown constant. Select $v_0 = 0$, then (3) can be reexpressed as

$$u(v) = g_0 v + g_2(v). \quad (5)$$

Then, one can further obtain

$$u^{p_n}(v) = g_0^{p_n} v^{p_n} + G(v) \quad (6)$$

where $G(v) = (g_0 v + g_2(v))^{p_n} - (g_0 v)^{p_n}$. Since $\lim_{v \rightarrow \infty} G(v) = 0$, which means that $G(v)$ is bound. Hence, there must be a constant $\bar{G} > 0$, such that $G(v) \leq \bar{G}$.

This article is to construct a novel DFPPC algorithm that ensures semi-global boundedness for all closed-loop signals, while ensuring that the system output accurately tracks the desired signal, and it consistently maintains the tracking error within the PCBs that are dependent on input and output constraints, where the PCBs will be given later in details.

A reasonable assumption is proposed to accomplish the above control objectives

Assumption 1 [7], [8]: The desired signal y_d and its first-order derivative is bounded and continuous.

Remark 1: Note that Assumption 1 is a standard assumption in tracking control problems, and similar assumption can be found in literatures like [7], [8], [9], [18], and [19]. In fact, the desired signal is usually designed by the path (or trajectory) planning algorithm, so its boundedness and differentiability are satisfied.

B. Important Lemmas

Lemma 1 [8]: The unknown nonlinear function $\bar{f}(\chi)$ can be approximated by an FLS as follows:

$$\bar{f}(\chi) = \Upsilon^T \Phi(\chi) + \epsilon(\chi), \quad (|\epsilon(\chi)| \leq \epsilon, \epsilon \in R^+) \quad (7)$$

where $\Phi(\chi)$, χ , Υ , $\epsilon(\chi)$ denote the basis function, input, weight and error of the FLS, respectively. $\Phi(\chi) =$

$[\phi_1(\chi), \dots, \phi_m(\chi)]^T / \sum_{i=1}^m \phi_i(\chi)$, $m > 1$ stands for the number of the fuzzy rules. Choose $\phi_i(\chi)$ as

$$\phi_i(\chi) = \exp\left[\frac{-(\chi - \zeta_i)^T(\chi - \zeta_i)}{l_i^2}\right], \quad i = 1, \dots, m$$

with l_i and ζ_i represent the center vector and the spreads of $\Phi_i(\chi)$.

Lemma 2 [9]: For $p \in R_{odd}^{\geq 1}$, $x, y \in R$, $m, n, \gamma \in R^+$, one has

$$|x^p - y^p| \leq p(2^{p-2} + 2)|x - y|(|x|^{p-1} + |y|^{p-1}) \quad (8)$$

$$|x|^m |y|^n \leq \frac{\gamma m}{m+n} |x|^{m+n} + \frac{n\gamma^{-\frac{m}{n}}}{m+n} |y|^{m+n}. \quad (9)$$

Lemma 3 [9]: For $m \geq 0$, $n > 0$ and $\gamma \geq 1$, we have

$$m \leq n + \left(\frac{m}{\gamma}\right)^\gamma \left(\frac{\gamma-1}{n}\right)^{\gamma-1}. \quad (10)$$

III. MAIN RESULTS

A. Dual Flexible PCBs

Inspired by [40], the following rate function (RF)-based initial performance function is introduced:

$$\mathcal{B}(\beta(t)) = \frac{\ell\beta(t)}{\sqrt{1-\beta^2(t)}} \quad (11)$$

where $\beta(t) = (\beta_0 - \beta_{t_s})\Gamma(t) + \beta_{t_s}$, ℓ , β_{t_s} , β_0 are the design parameters satisfying $0 < \beta_{t_s} < \beta_0 \leq 1$, $\ell > 0$. $\Gamma(t)$ denotes the RF, which has the following properties: 1) $\Gamma(0) = 1$ and $\Gamma(t) \in [0, 1) \forall t > 0$ and 2) $\Gamma^{(i)}(t)$ is bounded and piece-wise continuous with $i = 0, 1, \dots, n$. In this article, $\Gamma(t)$ is selected as follows:

$$\Gamma(t) = \begin{cases} \left(\frac{t_s-t}{t_s}\right)^{n+1}, & 0 \leq t < t_s \\ 0, & t \geq t_s \end{cases} \quad (12)$$

where t_s stands for a design constant, n represents the order of the system.

Design the following tensile model-based barrier function:

$$s = \frac{\zeta(t)}{(\delta_1 + \zeta(t))(\delta_2 - \zeta(t))} \quad (13)$$

where $0 < \delta_1, \delta_2 \leq 1$, $\tau \in R^+$ are the positive constants, $\zeta(t) = \eta(t)/\beta(t)$, $\eta(t) = N(\sigma)e_1/\sqrt{N^2(\sigma)e_1^2 + \ell^2}$, $e_1 = x_1 - y_d$ denotes the tracking error, $N(\sigma) = \exp(-\tau\sigma)$ denotes a tensile function, σ represents the output of the following auxiliary system:

$$\dot{\sigma} = -\rho_1\sigma + \rho_2(\kappa_1(t) + \kappa_2(t)), \quad \sigma(0) = 0 \quad (14)$$

where $\kappa_1(t) = (\text{sgn}(v - u_d) + 1)(v - u_d)$, $\kappa_2(t) = (\text{sgn}(v + u_d) - 1)(v + u_d)$, $\rho_1, \rho_2 \in R^+$.

Remark 2: It can be seen from the expressions of $\kappa_1(t)$ and $\kappa_2(t)$ that if and only if $|v| > u_d$, $\kappa_1(t) + \kappa_2(t) > 0$, and when $|v| \leq u_d$, $\kappa_1(t) + \kappa_2(t) \equiv 0$. Then, one can further know from (14) that when $|v| > u_d$, $\sigma > 0$, and when $|v| \leq u_d$, $\sigma = 0$. On the basis of the expression of $N(\cdot)$, one can further know that $N(\sigma) \in (0, 1]$, and if and only if $|v| \leq u_d$, $N(\sigma) = 1$.

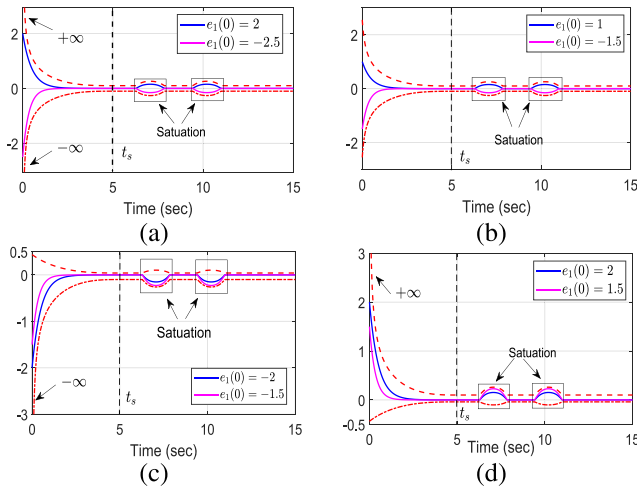


Fig. 1. Diagram of the corresponding dual flexible PCBs under different parameter selection. (a) $\delta_1 = \delta_2 = \beta_0 = 1$. (b) $0 < \delta_1, \delta_2, \beta_0 < 1$. (c) $\delta_2 = \beta_0 = 1, 0 < \delta_1 < 1$. (d) $\delta_1 = \beta_0 = 1, 0 < \delta_2 < 1$.

The dual flexible PCBs are design as follows:

$$\begin{cases} \underline{\mathcal{B}}(t) = \frac{\mathcal{B}(-\delta_1\beta(t))}{N(\sigma)} \\ \bar{\mathcal{B}}(t) = \frac{\mathcal{B}(\delta_2\beta(t))}{N(\sigma)} \end{cases} \quad (15)$$

where

$$\begin{cases} \mathcal{B}(-\delta_1\beta(t)) = \frac{-\ell\delta_1\beta(t)}{\sqrt{1-(\delta_1\beta(t))^2}} \\ \mathcal{B}(\delta_2\beta(t)) = \frac{\ell\delta_2\beta(t)}{\sqrt{1-(\delta_2\beta(t))^2}} \end{cases} \quad (16)$$

According to (13), one know that if $\zeta(0) \in (-\delta_1, \delta_2)$ and s is bounded, then $\zeta(t) \in (-\delta_1, \delta_2)$ holds for $\forall t \in R^+$. One can further obtain from the expression of $\zeta(t)$ that $\zeta(t) \in (-\delta_1, \delta_2)$ is equivalent to $\eta(t) \in (-\delta_1\beta(t), \delta_2\beta(t))$. Based on (11), we know that $\mathcal{B}(\cdot)$ is a strictly monotonically increasing function of \cdot , then $\eta(t) \in (-\delta_1\beta(t), \delta_2\beta(t))$ is further equivalent to

$$\mathcal{B}(-\delta_1\beta(t)) < \mathcal{B}(\eta(t)) < \mathcal{B}(\delta_2\beta(t)). \quad (17)$$

According to (17), one can obtain

$$\mathcal{B}(-\delta_1\beta(t)) < N(\sigma)e_1 < \mathcal{B}(\delta_2\beta(t)). \quad (18)$$

Based on (15) and (18), one has

$$\underline{\mathcal{B}}(t) < e_1 < \bar{\mathcal{B}}(t). \quad (19)$$

The above analysis shows that as long as $e_1(0) \in (\underline{\mathcal{B}}(0), \bar{\mathcal{B}}(0)) = (\mathcal{B}(-\delta_1\beta(0)), \mathcal{B}(\delta_2\beta(0)))$ and s is bounded, then $e_1(t) \in (\underline{\mathcal{B}}(t), \bar{\mathcal{B}}(t))$ holds for $\forall t \in R^+$, implying that the introduction of the barrier function (13) transforms the performance constraint control problem into the bounded control problem of s under the premise of satisfying the initial error constraint.

Remark 3: It is worth noting that the methods proposed in [50], [51], [52], [53], [54], and [55] also use the auxiliary system to build a balance between performance constraints and input saturation, under which there are actually two auxiliary systems, i.e., the output of one auxiliary system is always greater than or equal to 0, and that of other auxiliary system is always less than or equal to 0, then the outputs of two auxiliary

systems are added at the same time on the basis of the original upper and lower PCBs, so that when the input saturation occurs, the upper constraint boundary expands upward and the lower constraint boundary expands downward. Compared with the above methods, one of the most intuitive differences is that the designed auxiliary system (14) is more concise in form, which reduces the overall computational complexity to a certain extent. Note that the control goal of this article is to achieve “dual flexibility,” and it will be difficult to achieve the first flexibility goal if the direct addition or subtraction of the auxiliary system output is followed. To this end, this article innovatively designed the tensile model-based dual flexible PCBs (15), it is not difficult to see from (15) and the properties of $N(\sigma)$ that when input saturation occurs, the PCBs will expand adaptively; when $|v| \leq u_d$, $N(\sigma) = 1$, the PCBs will revert to the original PCBs.

Remark 4: Compare with SPPC methods [12], [13], [14], [15], [16], PTPPC methods [33], [34], [35], [36], [37], [38] for nonlinear systems without considering input saturation (i.e., $N(\sigma) \equiv 1$), and the FPPC methods [50], [51], [52], [53], [54], [55] for input saturated nonlinear systems, in which the initial PCBs are always bounded. However, the performance boundaries proposed in this article present a more flexible feature, i.e., the proposed approach can be adapted to the following different types of cases by adjusting the parameters.

- 1) Select $\delta_1 = \delta_2 = \beta_0 = 1$, it can be seen from (15) and (16) that $\underline{\mathcal{B}}(0) = \mathcal{B}(-\delta_1\beta(0)) = -\infty$ and $\bar{\mathcal{B}}(0) = \mathcal{B}(\delta_2\beta(0)) = +\infty$, i.e., $e_1(0) \in (-\infty, +\infty)$, which means that the proposed algorithm is suitable for the case where the initial error is completely unknown, see Fig. 1(a).
- 2) Select $0 < \delta_1, \delta_2, \beta_0 < 1$, it can be seen from (15) and (16) that $\underline{\mathcal{B}}(0) = \mathcal{B}(-\delta_1\beta(0)) = \underline{\mathcal{B}}$ and $\bar{\mathcal{B}}(0) = \mathcal{B}(\delta_2\beta(0)) = \bar{\mathcal{B}}$ ($\underline{\mathcal{B}}$ and $\bar{\mathcal{B}}$ stand for the bounded constants), i.e., $e_1(0) \in (\underline{\mathcal{B}}, \bar{\mathcal{B}})$. In this case, the proposed method is actually degraded to the traditional PTPPC method, see Fig. 1(b).
- 3) Select $\delta_2 = \beta_0 = 1, 0 < \delta_1 < 1$, it can be seen from (15) and (16) that $\underline{\mathcal{B}}(0) = \mathcal{B}(-\delta_1\beta(0)) = \underline{\mathcal{B}} < 0$ ($\underline{\mathcal{B}}$ stands for a bounded constant) and $\bar{\mathcal{B}}(0) = \mathcal{B}(\delta_2\beta(0)) = +\infty$, i.e., $e_1(0) \in (\underline{\mathcal{B}}, +\infty)$, which means that the proposed method is applicable to any scenario with $\text{sgn}(e_1(0)) = 1$, see Fig. 1(c).
- 4) Select $\delta_1 = \beta_0 = 1, 0 < \delta_2 < 1$, it can be seen from (15) and (16) that $\bar{\mathcal{B}}(0) = \mathcal{B}(\delta_2\beta(0)) = \bar{\mathcal{B}} > 0$ ($\bar{\mathcal{B}}$ stands for a bounded constant) and $\underline{\mathcal{B}}(0) = \mathcal{B}(-\delta_1\beta(0)) = -\infty$, i.e., $e_1(0) \in (-\infty, \bar{\mathcal{B}})$, which means that the proposed method is applicable to any scenario with $\text{sgn}(e_1(0)) = -1$, see Fig. 1(d).

Remark 5: Compare with the existing UPPC methods [40], [41], [42], [43] for nonlinear systems without considering the input saturation, and the PPC approaches of input saturated nonlinear systems [47], [48], [49], which either ignore input saturation or address the performance constraints and input saturation as separate issues, and assume that they can be implemented concurrently. In fact, performance constraints and input saturation often coexist, and the relationship between the two can mutually influence and interact with each other.

Therefore, the internal relationship between performance constraints and input saturation is innovatively established by introducing (14) and (15). According to (14), (15), and the expression of $N(\cdot)$, one know that when $|v| > u_d$ (i.e., the control input exceeds the saturation threshold), the range of PCBs can adaptively increase to mitigate the impact of input saturation on the tracking performance, so that the performance constraints are not violated; when $|v| \leq u_d$ (i.e., the control input is within the saturation threshold), the PCBs can adaptively revert back to the original PCBs [see Fig. 1(a)–(d)]. In other words, by designing the novel tensile model-based dual flexible PCBs (15), the proposed method establishes the relation between performance constraints and input saturation, thus achieving a balance between control performance (corresponding to performance constraints) and system security (corresponding to input saturation).

Remark 6: It needs to be emphasized that the proposed DFPPC method is actually a novel method that integrates the advantages of the existing advanced PPC methods (like PTPPC, UPPC and FPPC) into one, rather than a simple combination of the above methods. The PTPPC, UPPC and FPPC methods are both improvements and upgrades of SPPC method, which have their own advantages, but also have some shortcomings (see Remarks 4 and 5 for details). One of the biggest challenges of this article is how to design a unified control framework, which not only can be adapted to multiple types of initial errors by adjusting the parameters, but also can achieve a good balance between performance constraints and input saturation. This article innovatively proposes the tensile model-based barrier function (13) and the dual flexible PCBs (15) for the first time, which effectively overcomes the limitations of existing methods and realizes the dual flexibility.

B. Controller Design

From (15), we have

$$\dot{s} = \mu_1 \dot{e}_1 + \mu_2 \quad (20)$$

where

$$\mu_1 = \frac{(\delta_1 \delta_2 + \zeta^2) N \ell^2}{\beta (\delta_1 + \zeta)^2 (\delta_2 - \zeta)^2 (N^2 e_1^2 + \ell^2) \sqrt{N^2 e_1^2 + \ell^2}}$$

$$\mu_2 = \frac{(\delta_1 \delta_2 + \zeta^2) e_1 (\dot{N} - \eta N e_1 \dot{N} - \dot{\beta} \eta)}{\beta^2 (\delta_1 + \zeta)^2 (\delta_2 - \zeta)^2 \sqrt{N^2 e_1^2 + \ell^2}}$$

with $\zeta = \zeta(t)$, $N = N(\sigma(t))$, $\eta = \eta(t)$, $\beta = \beta(t)$.

Let $z_1 = s$, $z_i = x_i - \alpha_{i-1}$ with $i = 2, \dots, n$, α_i stands for the virtual control signal. $\Theta_i = \|\Upsilon_i\|^2$, $i = 1, 2, \dots, n$, Υ_i stands for the weight vector of FLS, $\tilde{\Theta}_i = \Theta_i - \hat{\Theta}_i$, $\hat{\Theta}_i$ denotes the estimate of Θ_i , $p = \max_{1 \leq i \leq n} \{p_i\}$, $P_i = p - p_i + 2$.

Step 1: The first Lyapunov function candidate (LFC) V_1 is selected as

$$V_1 = \frac{1}{P_1} z_1^{P_1} + \frac{1}{2r_1} \tilde{\Theta}_1^2 \quad (21)$$

where r_1 stands for a positive design parameter.

From (20)–(21), we have

$$\dot{V}_1 = z_1^{P_1-1} \bar{f}_1(\mathcal{Z}_1) + \mu_1 z_1^{P_1-1} (x_2^{p_1} - \alpha_1^{p_1}) + \mu_1 z_1^{P_1-1} \alpha_1^{p_1} - \frac{P_1-1}{P_1} z_1^{P_1} - \mu_1 \Xi_1 z_1^{p+1} - \frac{1}{r_1} \tilde{\Theta}_1 \dot{\hat{\Theta}}_1 \quad (22)$$

where $\bar{f}_1(\mathcal{Z}_1) = \mu_1(f_1(\bar{x}_1) - \dot{y}_d + \mu_2/\mu_1 + \Xi_1 z_1^{p_1}) + (P_1 - 1)z_1/\mu_1 P_1$, Ξ_1 will be given below.

It can be known from Lemma 1 that $\bar{f}_i(\mathcal{Z}_i)$ can be approximated by an FLS, i.e., $\bar{f}_i(\mathcal{Z}_i) = \epsilon_i(\mathcal{Z}_i) + \Upsilon_i^T \Phi_i(\mathcal{Z}_i)$, where $|\epsilon_i(\mathcal{Z}_i)| \leq \epsilon_i$ with $\epsilon_i \in R^+$.

According to Lemmas 2 and 3, we can obtain

$$z_1^{P_1-1} \bar{f}_1(\mathcal{Z}_1) = z_1^{P_1-1} (\epsilon_1(\mathcal{Z}_1) + \Upsilon_1^T \Phi_1(\mathcal{Z}_1))$$

$$\leq \frac{|z_1|^{P_1-1} \|\tilde{\Theta}_1\| \|\Phi_1(\mathcal{Z}_1)\|^2}{4a_1} + z_1^{p+1} \Psi_1$$

$$+ \frac{P_1-1}{P_1} z_1^{P_1} + \frac{\epsilon_1^{P_1}}{P_1} + \epsilon_1 \quad (23)$$

where $a_1, \epsilon_1 \in R^+$ stand for design parameters, and

$$\Psi_1 = \left[\frac{(P_1-1)\psi_1}{p+1} \right]^{\frac{p+1}{P_1-1}} \left[\frac{p_1}{(P_1-1)\epsilon_1} \right]^{\frac{P_1-1}{p}}$$

$$\psi_1 = \frac{\sqrt{1 + \hat{\Theta}_1^2} \|\Phi_1(\mathcal{Z}_1)\|^2}{4a_1} + a_1.$$

From Lemma 2, one has

$$\mu_1 z_1^{P_1-1} (x_2^{p_1} - \alpha_1^{p_1}) \leq \frac{p_1+1}{p+1} \mu_1 z_2^{p+1} + \Xi_1 \mu_1 z_1^{p+1} \quad (24)$$

where

$$\Xi_1 = \frac{(P_1-1)\xi_1^{\frac{p+1}{P_1-1}} + p(\xi_1 |\epsilon_1|^{p_1-1})^{\frac{p+1}{p}}}{p+1}$$

$$\xi_1 = p_1(2^{p_1-2} + 2).$$

α_1 and $\hat{\Theta}_1$ are designed as

$$\alpha_1 \triangleq -\Lambda_1 z_1 \quad (25)$$

$$\Lambda_1 = \left[\frac{1}{\mu_1} \left(\frac{\mathcal{C}_1}{P_1} c_1 + \Psi_1 \right) \right]^{\frac{1}{p_1}} \quad (26)$$

$$\dot{\hat{\Theta}}_1 = \frac{r_1 |z_1|^{P_1-1} \|\Phi_1(\mathcal{Z}_1)\|^2}{4a_1} - \gamma_1 \hat{\Theta}_1, \quad (\hat{\Theta}_1(0) > 0) \quad (27)$$

where c_1 and γ_1 denote the positive constants, and $\mathcal{C}_1 = P_1/(p+1)$.

Substituting (23)–(27) to (22), one has

$$\dot{V}_1 \leq -\frac{c_1 \mathcal{C}_1}{P_1} z_1^{p+1} + \frac{\gamma_1}{r_1} \tilde{\Theta}_1 \hat{\Theta}_1 + \frac{p_1+1}{p+1} \mu_1 z_2^{p+1} + d_1 \quad (28)$$

where $d_1 = \epsilon_1 + \epsilon_1^{P_1}/P_1$.

Step 2: The 2nd LFC V_2 is chosen as

$$V_2 = V_1 + \frac{1}{P_2} z_2^{P_2} + \frac{1}{2r_2} \tilde{\Theta}_2^2 \quad (29)$$

where r_2 stands for a positive design parameter.

Then, one can obtain

$$\begin{aligned} \dot{V}_2 \leq & -\frac{c_1 \mathcal{C}_1}{P_1} z_1^{p+1} + \frac{\gamma_1}{r_1} \tilde{\Theta}_1 \hat{\Theta}_1 + d_1 + z_2^{p_2-1} \bar{f}_2(\mathcal{Z}_2) \\ & + z_2^{p_2-1} (x_3^{p_2} - \alpha_2^{p_2}) + z_2^{p_2-1} \alpha_2^{p_2} - \Xi_2 z_2^{p+1} \\ & - \frac{P_2-1}{P_2} z_2^{p_2} - \frac{1}{r_2} \tilde{\Theta}_2 \dot{\hat{\Theta}}_2 \end{aligned} \quad (30)$$

where $\bar{f}_2(\mathcal{Z}_2) = [(p_1+1)\mu_1 z_2^{p_2}]/(p+1) + (P_2-1)z_2/P_2 + f_2(\bar{x}_2) + \Xi_2 z_2^{p_2} - \dot{\alpha}_1$, Ξ_2 will be shown below.

Similar to (23), one has

$$\begin{aligned} z_2^{p_2-1} \bar{f}_2(\mathcal{Z}_2) \leq & \frac{|z_2|^{p_2-1} \tilde{\Theta}_2 \|\Phi_2(\mathcal{Z}_2)\|^2}{4a_2} + z_2^{p+1} \Psi_2 \\ & + \frac{P_2-1}{P_2} z_2^{p_2} + \frac{\epsilon_2^{p_2}}{P_2} + \varepsilon_2 \end{aligned} \quad (31)$$

where a_2, ε_2 are positive design parameters, and

$$\begin{aligned} \Psi_2 &= \left[\frac{(P_2-1)\psi_2}{p+1} \right]^{\frac{p+1}{p_2-1}} \left[\frac{p_2}{(P_2-1)\varepsilon_2} \right]^{\frac{p_2}{p_2-1}} \\ &= \frac{\sqrt{1 + \hat{\Theta}_2^2} \|\Phi_2(\mathcal{Z}_2)\|^2}{4a_2} + a_2. \end{aligned}$$

From Lemma 2, one has

$$z_2^{p_2-1} (x_3^{p_2} - \alpha_2^{p_2}) \leq \frac{p_2+1}{p+1} z_3^{p+1} + \Xi_2 z_2^{p+1} \quad (32)$$

where

$$\begin{aligned} \Xi_2 &= \frac{(P_2-1)\xi_2^{\frac{p+1}{p_2-1}} + p(\xi_2|\epsilon_2|^{p_2-1})^{\frac{p+1}{p}}}{p+1} \\ \xi_2 &= p_2(2^{p_2-2} + 2). \end{aligned}$$

Design α_2 and $\hat{\Theta}_2$ as

$$\alpha_2 \triangleq -\Lambda_2 z_2 \quad (33)$$

$$\Lambda_2 = \left(\frac{\mathcal{C}_2}{P_2} c_2 + \Psi_2 \right)^{\frac{1}{p_2}} \quad (34)$$

$$\dot{\hat{\Theta}}_2 = \frac{r_2 |z_2|^{p_2-1} \|\Phi_2(\mathcal{Z}_2)\|^2}{4a_2} - \gamma_2 \hat{\Theta}_2, (\hat{\Theta}_2(0) > 0) \quad (35)$$

where c_2 and γ_2 denote the positive constants, and $\mathcal{C}_2 = P_2/(p+1)$.

Substituting (31)–(35) to (30), one has

$$\dot{V}_2 \leq -\sum_{j=1}^2 \left(\frac{c_j \mathcal{C}_j}{P_j} z_j^{p+1} - \frac{\gamma_j}{r_j} \tilde{\Theta}_j \hat{\Theta}_j - d_j \right) + \frac{p_2+1}{p+1} z_3^{p+1} \quad (36)$$

where $d_j = \varepsilon_j + \epsilon_j^{p_j}/P_j$.

Step i ($i = 3, \dots, n-1$): The i th LFc V_i is selected as

$$V_i = V_{i-1} + \frac{1}{P_i} z_i^{p_i} + \frac{1}{2r_i} \tilde{\Theta}_i^2 + V_{i-1}, \quad (r_i \in R^+). \quad (37)$$

It can be obtain from (37) that

$$\begin{aligned} \dot{V}_i &= -\sum_{j=1}^{i-1} \left(\frac{c_j \mathcal{C}_j}{P_j} z_j^{p+1} - \frac{\gamma_j}{r_j} \tilde{\Theta}_j \hat{\Theta}_j - d_j \right) + z_i^{p_i-1} \bar{f}_i(\mathcal{Z}_i) \\ &+ z_i^{p_i-1} (x_{i+1}^{p_i} - \alpha_i^{p_i}) + z_i^{p_i-1} \alpha_i^{p_i} - \Xi_i z_i^{p+1} \end{aligned}$$

$$- \frac{P_i-1}{P_i} z_i^{p_i} - \frac{1}{r_i} \tilde{\Theta}_i \dot{\hat{\Theta}}_i \quad (38)$$

where $\bar{f}_i(\mathcal{Z}_i) = [(p_{i-1}+1)z_i^{p_i}]/(p+1) + (P_i-1)z_i/P_i + f_i(\bar{x}_i) + \Xi_i z_i^{p_i} - \dot{\alpha}_{i-1}$, Ξ_i will be shown below.

According to Lemmas 2 and 3, one has

$$\begin{aligned} z_i^{p_i-1} \bar{f}_i(\mathcal{Z}_i) \leq & \frac{|z_i|^{p_i-1} \tilde{\Theta}_i \|\Phi_i(\mathcal{Z}_i)\|^2}{4a_i} + z_i^{p+1} \Psi_i \\ & + \frac{P_i-1}{P_i} z_i^{p_i} + \frac{\Delta_i^{P_i}}{P_i} + \varepsilon_i \end{aligned} \quad (39)$$

where $\varepsilon_i, a_i \in R^+$ stand for the design constants, and

$$\begin{aligned} \Psi_i &= \left[\frac{(P_i-1)\psi_i}{p+1} \right]^{\frac{p+1}{p_i-1}} \left[\frac{p_i}{(P_i-1)\varepsilon_i} \right]^{\frac{p_i}{p_i-1}} \\ \psi_i &= \frac{\sqrt{1 + \hat{\Theta}_i^2} \|\Phi_i(\mathcal{Z}_i)\|^2}{4a_i} + a_i. \end{aligned}$$

Based on Lemma 2, we have

$$z_i^{p_i-1} (x_{i+1}^{p_i} - \alpha_i^{p_i}) \leq \frac{p_i+1}{p+1} z_{i+1}^{p+1} + \Xi_i z_i^{p+1} \quad (40)$$

where

$$\begin{aligned} \Xi_i &= \frac{p(\xi_i|\epsilon_i|^{p_i-1})^{\frac{p+1}{p}} + (P_i-1)\xi_i^{\frac{p+1}{p_i-1}}}{p+1} \\ \xi_i &= p_i(2^{p_i-2} + 2). \end{aligned}$$

Construct α_i and $\hat{\Theta}_i$ as

$$\alpha_i \triangleq -\Lambda_i z_i \quad (41)$$

$$\Lambda_i = \left(\frac{\mathcal{C}_i}{P_i} c_i + \Psi_i \right)^{\frac{1}{p_i}} \quad (42)$$

$$\dot{\hat{\Theta}}_i = \frac{r_i |z_n|^{p_i-1} \|\Phi_i(\mathcal{Z}_i)\|^2}{4a_i} - \gamma_i \hat{\Theta}_i, (\hat{\Theta}_i(0) > 0) \quad (43)$$

where c_i and γ_i denote the positive constants, and $\mathcal{C}_i = P_i/(p+1)$.

Substituting (39)–(43) to (38), one has

$$\dot{V}_i \leq -\sum_{j=1}^i \left(\frac{c_j \mathcal{C}_j}{P_j} z_j^{p+1} - \frac{\gamma_j}{r_j} \tilde{\Theta}_j \hat{\Theta}_j - d_j \right) + \frac{p_i+1}{p+1} z_{i+1}^{p+1}. \quad (44)$$

Step n : The n th LFc V_n is selected as

$$V_n = V_{n-1} + \frac{1}{g} z_n^{p_n} + \frac{1}{2r_n} \tilde{\Theta}_n^2, \quad (r_n \in R^+). \quad (45)$$

According to (45), we have

$$\begin{aligned} \dot{V}_n &\leq -\sum_{j=1}^{n-1} \left(\frac{c_j \mathcal{C}_j}{P_j} z_j^{p+1} - \frac{\gamma_j}{r_j} \tilde{\Theta}_j \hat{\Theta}_j - d_j \right) - \frac{1}{r_n} \tilde{\Theta}_n \dot{\hat{\Theta}}_n \\ &+ \frac{1}{g} z_n^{p_n-1} (g_0^{p_n} v^{p_n} + G(v) + f_n(\bar{x}_n) - \dot{\alpha}_{n-1}) \\ &+ \frac{p_{n-1}+1}{p+1} z_n^{p+1}. \end{aligned} \quad (46)$$

From (9), one has

$$\frac{1}{g} z_n^{p_n-1} G(v) \leq \frac{2^{p_n-2}}{4g} + \frac{\bar{G}^2}{g}. \quad (47)$$

Then, we have

$$\begin{aligned} \dot{V}_n \leq & - \sum_{j=1}^{n-1} \left(\frac{c_j \mathcal{C}_j}{P_j} z_j^{p+1} - \frac{\gamma_j \tilde{\Theta}_j \hat{\Theta}_j}{r_j} - d_j \right) - \frac{1}{r_n} \tilde{\Theta}_n \dot{\hat{\Theta}}_n \\ & + z_n^{P_n-1} \bar{f}_n(\mathcal{Z}_n) + \frac{z_n^{P_n-1} g_0^{P_n} v^{P_n}}{g} + \frac{\bar{G}^2}{g} \\ & - \frac{P_n - 1}{P_n} z_n^{P_n} \end{aligned} \quad (48)$$

where $\bar{f}_n(\mathcal{Z}_n) = (f_n(\bar{x}_n) - \dot{\alpha}_{n-1} + z_n^{P_n-1}/4)/g + [(p_{n-1} + 1)z_n^{p_n}]/(p+1) + (P_n - 1)z_n/P_n$

According to Lemmas 2 and 3, one has

$$\begin{aligned} z_n^{P_n-1} \bar{f}_n(\mathcal{Z}_n) \leq & z_n^{p+1} \Psi_n + \frac{|z_n|^{P_n-1} \tilde{\Theta}_n \|\Phi_n(\mathcal{Z}_n)\|^2}{4a_n} \\ & + \frac{P_n - 1}{P_n} z_n^{P_n} + \frac{\epsilon_n^{P_n}}{P_n} + \varepsilon_n \end{aligned} \quad (49)$$

where $\varepsilon_n, a_n \in R^+$ stand for the design constants, and

$$\begin{aligned} \Psi_n &= \left[\frac{(P_n - 1)\psi_n}{p+1} \right]^{\frac{p+1}{P_n-1}} \left[\frac{p_n}{(P_n - 1)\varepsilon_n} \right]^{\frac{P_n}{P_n-1}} \\ \psi_n &= \frac{\sqrt{1 + \hat{\Theta}_n^2 \|\Phi_n(\mathcal{Z}_n)\|^2}}{4a_n} + a_n. \end{aligned}$$

Design v and $\dot{\hat{\Theta}}_n$ as

$$v = -\Lambda_n z_n \quad (50)$$

$$\Lambda_n = \left(\frac{\mathcal{C}_n}{P_n} c_n + \Psi_n \right)^{\frac{1}{p_n}} \quad (51)$$

$$\dot{\hat{\Theta}}_n = \frac{r_n |z_n|^{P_n-1} \|\Phi_n(\mathcal{Z}_n)\|^2}{4a_n} - \gamma_n \hat{\Theta}_n, \quad \hat{\Theta}_n(0) > 0 \quad (52)$$

where c_n and γ_n denote the positive constants, $\mathcal{C}_n = P_n/(p+1)$.

Substituting (47)–(52) to (46), one can obtain

$$\dot{V}_n \leq - \sum_{j=1}^n \left(\frac{c_j \mathcal{C}_j}{P_j} z_j^{p+1} - \frac{\gamma_j \tilde{\Theta}_j \hat{\Theta}_j}{r_j} - d_j \right) + \frac{\bar{G}^2}{g}. \quad (53)$$

It can be obtained from Lemma 3 that $z_i^{P_i} \leq (p_i - 1)/(p+1) + \mathcal{C}_i z_i^{p+1}$, then $-z_i^{P_i} \leq (-z_i^{p_i} + (p_i - 1)/(p+1))/\mathcal{C}_i, i = 1, \dots, n$. Then, we can further obtain

$$\dot{V}_n \leq - \sum_{j=1}^n \left[\frac{c_j}{P_j} z_j^p - \frac{\gamma_j \tilde{\Theta}_j \hat{\Theta}_j}{r_j} - (d_j + \frac{b_j}{\mathcal{C}_j}) \right] + \frac{\bar{G}^2}{g}. \quad (54)$$

According to $\tilde{\Theta}_j \hat{\Theta}_j \leq -\tilde{\Theta}_j^2/2 + \Theta_j^2/2$, one has

$$\dot{V}_n \leq - \sum_{j=1}^n \frac{c_j}{P_j} z_j^p - \sum_{j=1}^n \frac{\gamma_j \tilde{\Theta}_j^2}{2r_j} + d \quad (55)$$

where $d = \sum_{j=1}^n (d_j + b_j/\mathcal{C}_j) + \sum_{j=1}^n \gamma_j \Theta_j^2/2r_j + \bar{G}^2/g$.

Fig. 2 gives the block diagram of the proposed DFPPC algorithm.

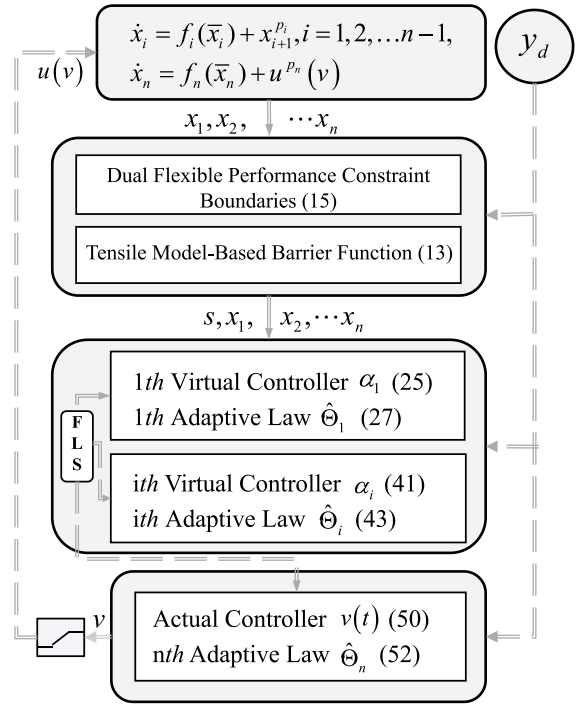


Fig. 2. Block diagram of the presented SFPPC algorithm.

C. Stability Analysis

Theorem: Consider the IS-HONSSs (1) with $e_1(0) \in (\underline{\mathcal{B}}(0), \bar{\mathcal{B}}(0))$, the constructed DFPPC algorithm ensures that:

- 1) the closed-loop signals are semi-globally bounded and
- 2) the system output is capable of effectively tracking the desired signal, while ensuring that the tracking error e_1 remains consistently within the dual flexible PCBs determined by both output and input constraints, i.e., $e(t) \in (\underline{\mathcal{B}}(t), \bar{\mathcal{B}}(t))$.

Proof:

1) The entire LF is selected as $V = V_n$. Let $c = \min_{1 \leq j \leq n} \{c_j, 2\gamma_j\}$, we can obtain from (55) that

$$\dot{V} \leq -cV + d. \quad (56)$$

According to (56), one can further obtain

$$V \leq V(0) + \frac{d}{c}. \quad (57)$$

Based on the expression of V , one has

$$|z_i| \leq \left[P_i \left(V(0) + \frac{d}{c} \right) \right]^{\frac{1}{P_i}} \quad (58)$$

$$|\tilde{\Theta}_i| \leq \sqrt{2r_i \left(V(0) + \frac{d}{c} \right)}. \quad (59)$$

One can know from (58) and (59) that $\tilde{\Theta}_i$ and z_i are bounded. According to (25), (33), (41), and (50), one can further know that α_i and v are bounded, then x_i is also bounded. Sum up, all of the closed-loop signals are bounded.

2) $e_1(0) \in (\underline{\mathcal{B}}(0), \bar{\mathcal{B}}(0))$ means that $e_1(0) \in (\mathcal{B}(-\delta_1 \beta(0)), \mathcal{B}(\delta_2 \beta(0)))$. On the basis of (13)–(18) and the boundedness of s , one can further know that $e_1(t) \in$

$(\mathcal{B}(-\delta_1\beta(t))/N(\sigma), \mathcal{B}(\delta_2\beta(t)/N(\sigma)))$ holds for $\forall t \in R^+$, i.e., $e_1(t) \in (\underline{\mathcal{B}}(t), \bar{\mathcal{B}}(t))$ holds for $\forall t \in R^+$. According to the properties of $\mathcal{B}(\cdot)$ and $\beta(t)$, one can further obtain that $e_1(t) \in (\mathcal{B}(-\delta_1\beta_{t_s})/N(\sigma), \mathcal{B}(\delta_2\beta_{t_s}/N(\sigma)))$ for $\forall t \geq t_s$, where $\mathcal{B}(-\delta_1\beta_{t_s})$ and $\mathcal{B}(\delta_2\beta_{t_s})$ are constants. The above indicates that the system output is capable of effectively tracking the desired signal, and $e_1(t)$ remains consistently within the dual flexible PCBs determined by both output and input constraints. In particular, if input saturation is not considered (i.e., $N(\sigma) = 1$), then $e_1(t) \in (\mathcal{B}(-\delta_1\beta_{t_s}), \mathcal{B}(\delta_2\beta_{t_s}))$ for $\forall t \geq t_s$, meaning that, in this case, the proposed method can achieve prescribed time convergence. ■

Remark 7: Note that the proposed method is an intelligent control method, and the designed controller does not involve the expression of specific system functions, meaning that the proposed method is suitable for IS-HONSs with uncertain models. In the control design, the FLSs are used to approximate the uncertain nonlinear terms. This is fundamentally different from the traditional control methods, i.e., the proposed method does not completely depend on the system model. From this point of view, the presented method has certain reference value for model-free control algorithms.

Remark 8: It should be pointed out that in order to achieve dual flexibility, the proposed DFPPC algorithm involves some parameters. The selection of parameters usually follows the following rules: 1) the design rules of $\beta_0, t_s, \beta_{t_s}, l$ are similar to the conventional UPPC method (see [28], [40] for details) and 2) τ is to control the expansion of the constrained boundary when input saturation occurs, and the larger the τ , the smaller the expansion. Of course, the pursuit of extreme performance also increases the complexity of algorithm design and calculation to a certain extent.

Remark 9: It is worth noting that this article considers the symmetric input saturation, and it can actually be further extended to asymmetric case. Let u_{ud} and u_{ld} as the upper and lower saturation thresholds, respectively, and replace (2) with: $u(v) = v$ when $u_{ld} < v < u_{ud}$, $u(v) = u_{ud}$ when $v \geq u_{ud}$, and $u(v) = u_{ld}$ when $v \leq u_{ld}$; $g_1(v)$ in (3) is replaced by: $g_1(v) = u_{ud} \tanh(v/u_{ud})$ when $v \geq 0$, and $g_1(v) = u_{ld} \tanh(v/u_{ld})$ when $v < 0$, then $|g_2(v)| \leq \max\{u_{ud}(1 - \tanh(1)), u_{ld}(\tanh(1) - 1)\} = \bar{g}$; $\kappa_1(t)$ and $\kappa_2(t)$ in (14) are replaced by: $\kappa_1(t) = (\text{sgn}(v - u_{ud}) + 1)(v - u_{ud})$, $\kappa_2(t) = (\text{sgn}(v + u_{ld}) - 1)(v + u_{ld})$. Then, the proposed algorithm is extended to DFPPC for HONSs with asymmetric input saturation. In addition, according to (55) and (58), one know that d contains the upper bound of G , which means that the introduction of G will increase the convergence region to some extent. Of course, since the PPC is introduced in this article, the convergence domain of tracking error actually depends more on the value of the PCBs, so the influence of G on the convergence domain is weakened to a certain extent.

Remark 10: It is worth noting that the proposed algorithm can actually ensure that the system output can track the reference signal with the prescribed accuracy within the prescribed time if and only if the input saturation is not considered. It can be seen from (15) that when input saturation is not considered (i.e., $N(\sigma) = 1$), the PCBs are constants when $t \geq t_s$, meaning that the prescribed time convergence can be achieved in this

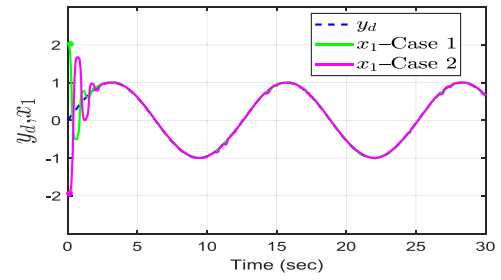


Fig. 3. Tracking curves under two different initial errors.

case. However, when input saturation is considered, once input saturation occurs, the PCBs will adaptively expand to avoid singularity, and when the control input returns to the threshold range, the PCBs will return to the original PCBs in the form of exponential convergence. Strictly speaking, in this case, the prescribed time convergence cannot be fully achieved.

IV. SIMULATION

Example 1: The following IS-HONS is considered:

$$\begin{cases} \dot{x}_1 = x_1 \sin x_1 + x_2^3, \\ \dot{x}_2 = -0.4x_1^2 - 0.4x_2^2 \cos x_2 + u^3(v), \\ y = x_1. \end{cases} \quad (60)$$

Let $y_d = \sin(0.5t)$, $t_s = 5$, $\beta_{t_s} = 0.06$, $\ell = 1$, $\tau = 0.2$, $\rho_1 = 5$, $\rho_2 = 0.5$, $u_d = 2$, $c_i = 40$, $\gamma_i = 3$, $r_i = 0.1$, $a_i = 10$ with $i = 1, 2$, $[\hat{\Theta}_1(0), \hat{\Theta}_2(0)]^T = [3, 4]^T$. Let $\beta_0 = \delta_i = 1$, it can be seen from (16) that in this case the initial PCBs are infinite, i.e., $\underline{\mathcal{B}}(0) = -\infty$ and $\bar{\mathcal{B}}(0) = +\infty$, which means that the proposed DFPPC algorithm is suitable for the case where the initial error is completely unknown. To verify this, we chose two initial error cases: 1) case 1 $e_1(0) = 2$ and 2) case 2 $e_1(0) = -2$. Figs. 3 and 4, respectively, give the tracking curves, tracking error curves and control input curves in two cases, showing that the proposed DFPPC method can ensure that the system output is capable of effectively tracking the desired signal, while ensuring that the tracking error e_1 remains consistently within the dual flexible PCBs determined by both output and input constraints.

In order to verify the flexibility of this method, we select three different sets of parameters for three different initial errors: *Case 1:* $e_1(0) = 1.5$, $\delta_1 = 0.5$, $\beta_0 = \delta_2 = 1$; *Case 2:* $e_1(0) = -1.5$, $\delta_2 = 0.5$, $\beta_0 = \delta_1 = 1$; and *Case 3:* $e_1(0) = 0.5$, $\delta_1 = \delta_2 = 0.5$, $\beta_0 = 0.9$. Fig. 5(a) gives the tracking curves in three cases, and Fig. 5(b)–(d), respectively, give the tracking curves in three cases, showing that the proposed method can be adapted to the different types of cases by adjusting the parameters.

The proposed DFPPC method is compared with the SPPC method [16] in order to validate its superiority, assuming that input saturation is not considered, i.e., $u(v) \equiv v$. Fig. 6(a) and (b) shows the tracking error curves of the SPPC algorithm in [16] and the proposed DFPPC algorithm, respectively. Obviously, since the initial PCBs of the SPPC method must be bounded, it is only applicable to the case where the initial error is within the PCBs (such as $e_1(0) = 1.5$), but not to other cases (like $e_1(0) = 3$ and $e_1(0) = -3$), while the DFPPC

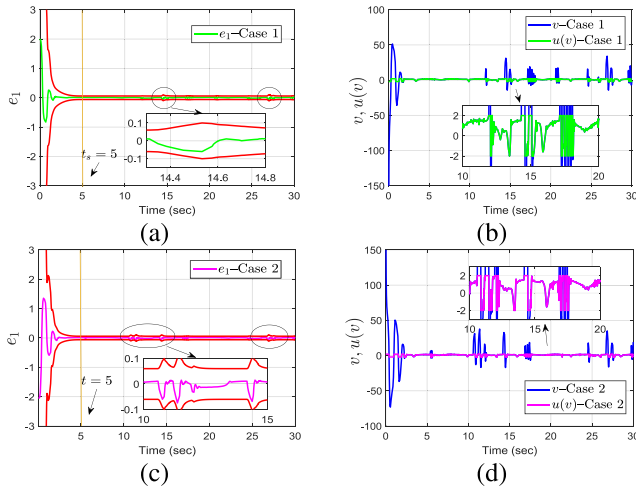


Fig. 4. (a) and (b), respectively, represents the tracking curve and control input curve in case 1. (c) and (d), respectively, represents the tracking curve and control input curve in case 2.

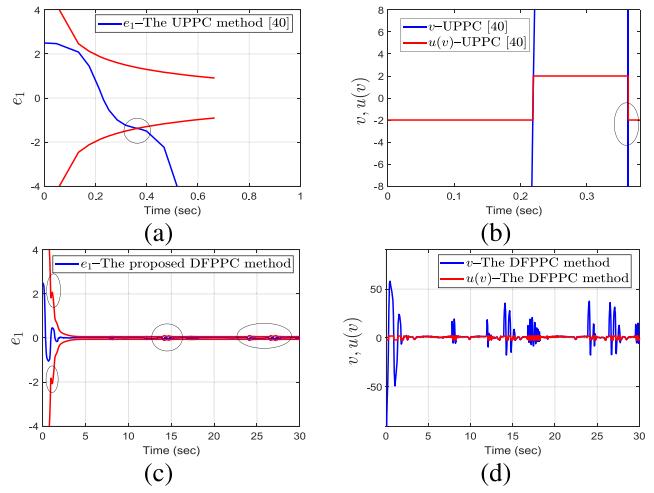


Fig. 7. (a) and (b), respectively, represent the tracking error curve and control input curve under the action of the UPPC method [40]. (c) and (d), respectively, represent the tracking error curve and control input curve under the action of the proposed DFPPC method.

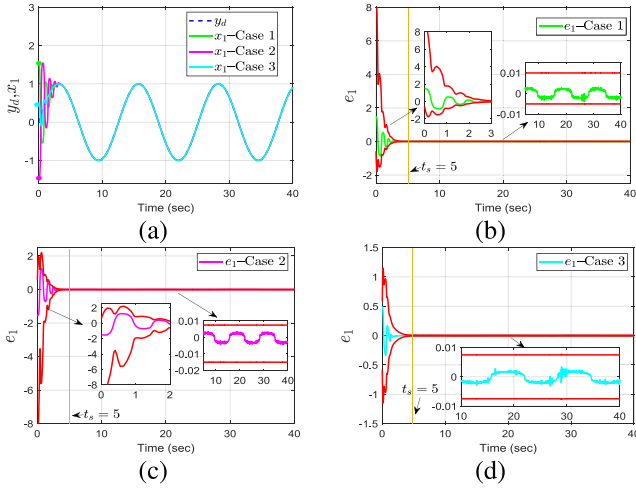


Fig. 5. (a) Represent the tracking curves in three cases. (b)–(d), respectively, represent the tracking curves in three cases.

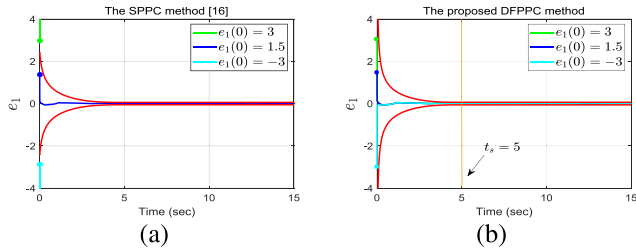


Fig. 6. (a) Tracking error curve under the action of the SPPC method [16] under three different initial errors. (b) Tracking error curve under the action of the proposed DFPPC method under three different initial errors.

algorithm proposed in this article is applicable to the three different initial errors.

The proposed DFPPC method is further compared with the UPPC method in [40] to underscore its superior performance. It is worth noting that the UPPC method proposed in [40] can be also applied to a variety of different initial error cases by adjusting parameters. However, this approach ignores the input saturation that is widespread in real systems. One

can see from Fig. 6(a) and (b) that when the control input exceeds the saturation threshold, the tracking performance will weaken and even exceed the PCBs, resulting in the failure of simulation to continue. However, this article innovatively establishes an internal relationship between performance constraints and input saturation (see Remark 5 for details), it can be seen from Fig. 6(c) and (d) that when $|v| > u_d$, the range of PCBs can adaptively increase to mitigate the impact of input saturation on the tracking performance, so that the performance constraints are not violated; when $|v| \leq u_d$, the PCBs can adaptively revert back to the original PCBs. From this perspective, the proposed DFPPC approach strikes a good balance between security performance and tracking performance.

Example 2: Consider the following simplified boiler unit model [9]:

$$\begin{cases} \dot{x}_1 = x_2^3 \\ \dot{x}_2 = \frac{x_1^2}{1+x_2^2} + u(v) \\ y = x_1 \end{cases} \quad (61)$$

where v , x_1 and x_2 represent the position of the control valve, the drum and reheater pressures, respectively. Let $y_d = \sin(0.5t) + 0.5 \sin t$, $t_s = 5$, $\beta_{t_s} = 0.06$, $\ell = 1$, $\tau = 0.2$, $\rho_1 = 5$, $\rho_2 = 0.5$, $u_d = 5$, $c_i = 40$, $\gamma_i = 3$, $r_i = 0.1$, $a_i = 10$ with $i = 1, 2$, $[\hat{\theta}_1(0), \hat{\theta}_2(0)]^T = [3, 4]^T$. Let $\beta_0 = \delta_i = 1$, it can be seen from (16) that in this case the initial PCBs are infinite, i.e., $\underline{\beta}(0) = -\infty$ and $\bar{\beta}(0) = +\infty$. We chose two initial error cases: 1) case 1 $e_1(0) = 2$ and 2) case 2 $e_1(0) = -2$. Figs. 8 and 9, respectively, give the tracking curves, tracking error curves and control input curves in two cases, showing that the proposed method can ensure that the system output can track the desired signal, and e_1 always kept within the dual flexible PCBs that depend on output and input constraints.

In order to verify the flexibility of this method, we select three different sets of parameters for three different initial errors: 1) *Case 1:* $e_1(0) = 1.5$, $\delta_1 = 0.5$, $\beta_0 = \delta_2 = 1$; 2) *Case 2:* $e_1(0) = -1.5$, $\delta_2 = 0.5$, $\beta_0 = \delta_1 = 1$; and

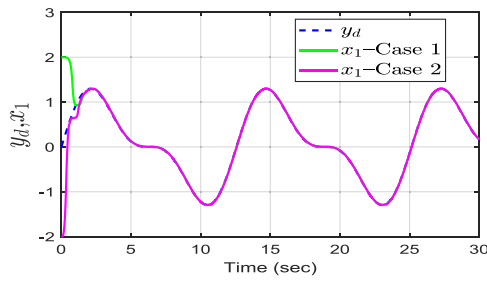


Fig. 8. Tracking curves under two different initial errors.

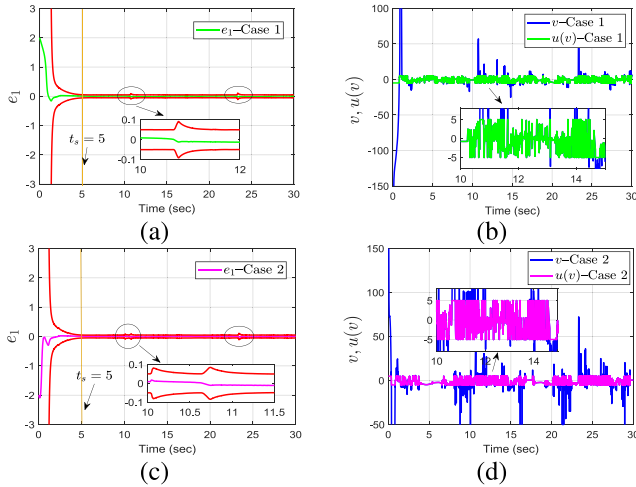


Fig. 9. (a) and (b), respectively, represents the tracking curve and control input curve in case 1. (c) and (d), respectively, represents the tracking curve and control input curve in case 2.

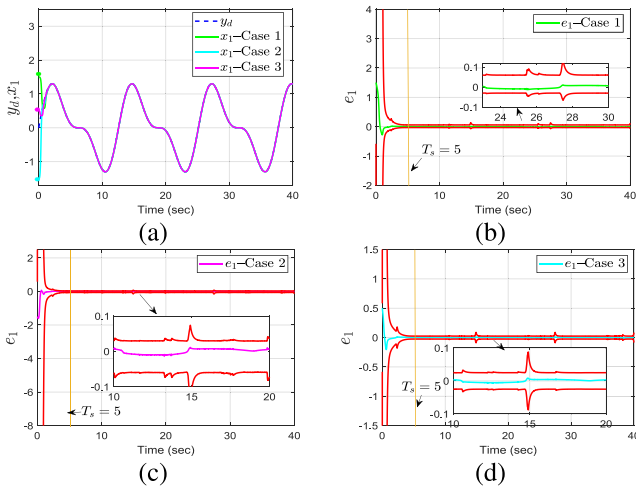


Fig. 10. (a) Represent the tracking curves in three cases. (b)–(d), respectively, represent the tracking curves in three cases.

Case 3: $e_1(0) = 0.5, \delta_1 = \delta_2 = 0.5, \beta_0 = 0.9$. Fig. 10(a) gives the tracking curves in three cases, and Fig. 10(b)–(d), respectively, give the tracking curves in three cases, showing that the proposed method can be adapted to the different types of cases by adjusting the parameters.

The proposed DFPPC method is compared with the SPPC method [16] in order to validate its superiority, assuming that input saturation is not considered, i.e., $u(v) \equiv v$.

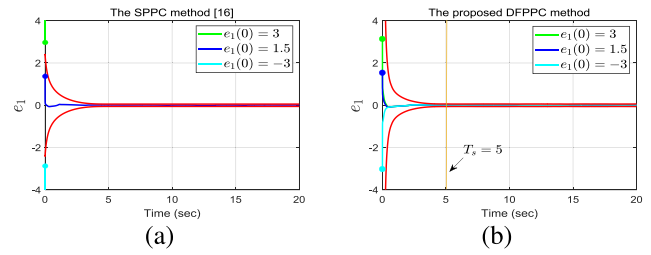


Fig. 11. (a) Tracking error curve under the action of the SPPC method [16] under three different initial errors. (b) Tracking error curve under the action of the proposed DFPPC method under three different initial errors.

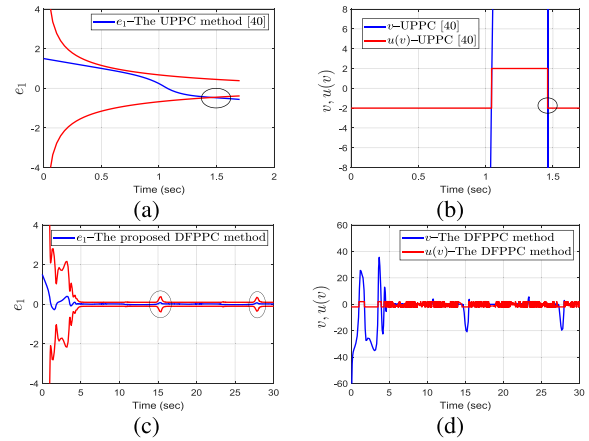


Fig. 12. (a) and (b), respectively, represent the tracking error curve and control input curve under the action of the UPPC method [40]. (c) and (d), respectively, represent the tracking error curve and control input curve under the action of the proposed DFPPC method.

Fig. 11(a) and (b) shows the tracking error curves of the SPPC algorithm in [16] and the proposed DFPPC algorithm, respectively. One can know from Fig. 11(a) that the SPPC method is only applicable to the case where the initial error is within the PCBs (such as $e_1(0) = 1.5$), but not to other cases (like $e_1(0) = 3$ and $e_1(0) = -3$), while the proposed DFPPC algorithm is suitable for the three different initial errors.

The proposed DFPPC method is further compared with the UPPC method in [40] to underscore its superior performance. From Fig. 12(a) and (b), one know that when the control input exceeds the saturation threshold, the tracking performance will weaken and even exceed the PCBs, resulting in the failure of simulation to continue. However, one can see from Fig. 12(c) and (d) that when $|v| > u_d$, the range of PCBs can adaptively increase to mitigate the impact of input saturation on the tracking performance, so that the performance constraints are not violated; when $|v| \leq u_d$, the PCBs can adaptively revert back to the original PCBs, implying that the DFPPC approach proposed in this article strikes a good balance between security performance and tracking performance.

V. CONCLUSION

A novel DFPPC algorithm for IS-HONSs is presented in this article. The difference from the existing PPC methods is that the proposed DFPPC algorithm not only can be adapted to multiple types of initial errors by adjusting the parameters,

but also can achieve a good balance between input saturation and performance constraints. The results demonstrate that the DFPPC algorithm proposed in this article guarantees semi-global boundedness for all closed-loop signals, while ensuring that the system output accurately tracks the desired signal, and it consistently maintains the tracking error within dual flexible PCBs that are dependent on input and output constraints. The future research will primarily concentrate on the event-triggered-based DFPPC algorithm [58], [59] for IS-HONSS under DoS attacks.

REFERENCES

- [1] K. B. Ngo, R. Mahony, and Z.-P. Jiang, "Integrator backstepping using barrier functions for systems with multiple state constraints," in *Proc. 44th IEEE Conf. Decision Control*, 2005, pp. 8306–8312.
- [2] Y. Liu, Y. Wang, Y. Feng, and Y. Wu, "Neural network-based adaptive boundary control of a flexible riser with input deadzone and output constraint," *IEEE Trans. Cybern.*, vol. 52, no. 12, pp. 13120–13128, Dec. 2022.
- [3] S. Ding, B. Zhang, K. Mei, and J. H. Park, "Adaptive fuzzy SOSM controller design with output constraints," *IEEE Trans. Fuzzy Syst.*, vol. 30, no. 7, pp. 2300–2311, Jul. 2022.
- [4] Y. Mei, Y. Liu, H. Wang, and H. Cai, "Adaptive deformation control of a flexible variable-length rotary crane arm with asymmetric input-output constraints," *IEEE Trans. Cybern.*, vol. 52, no. 12, pp. 13752–13761, Dec. 2022.
- [5] Y. Liu, X. Chen, Y. Wu, H. Cai, and H. Yokoi, "Adaptive neural network control of a flexible spacecraft subject to input nonlinearity and asymmetric output constraint," *IEEE Trans. Neural Netw. Learn. Syst.*, vol. 33, no. 11, pp. 6226–6234, Nov. 2022.
- [6] K. Zhao and Y. Song, "Removing the feasibility conditions imposed on tracking control designs for state-constrained strict-feedback systems," *IEEE Trans. Autom. Control*, vol. 64, no. 3, pp. 1265–1272, Mar. 2019.
- [7] K. Zhao, L. Chen, and C. L. P. Chen, "Event-based adaptive neural control of nonlinear systems with deferred constraint," *IEEE Trans. Syst., Man, Cybern., Syst.*, vol. 52, no. 10, pp. 6273–6282, Oct. 2022.
- [8] Y. Yao, J. Tan, J. Wu, and X. Zhang, "A unified fuzzy control approach for stochastic high-order nonlinear systems with or without state constraints," *IEEE Trans. Fuzzy Syst.*, vol. 30, no. 10, pp. 4530–4540, Oct. 2022.
- [9] Y. Yao, Y. Kang, Y. Zhao, P. Li, and J. Tan, "Unified fuzzy control of high-order nonlinear systems with multi-type state constraints," *IEEE Trans. Cybern.*, vol. 54, no. 4, pp. 2525–2535, Apr. 2024.
- [10] Y. Yao, J. Tan, J. Wu, and X. Zhang, "Decentralized fixed-time control for state-constrained stochastic systems via nonlinear state-dependent function approach," *Int. J. Robust Nonlinear Control*, vol. 32, no. 8, pp. 4923–4945, 2022.
- [11] Y. Yao, J. Tan, J. Wu, and X. Zhang, "Event-triggered fixed-time adaptive fuzzy control for state-constrained stochastic nonlinear systems without feasibility conditions," *Nonlinear Dyn.*, vol. 105, pp. 403–416, Jun. 2021.
- [12] C. P. Bechlioulis and G. A. Rovithakis, "Robust adaptive control of feedback linearizable MIMO nonlinear systems with prescribed performance," *IEEE Trans. Autom. Control*, vol. 53, no. 9, pp. 2090–2099, Oct. 2008.
- [13] Y. Liu and H. Ma, "Adaptive fuzzy tracking control of nonlinear switched stochastic systems with prescribed performance and unknown control directions," *IEEE Trans. Syst., Man, Cybern., Syst.*, vol. 50, no. 2, pp. 590–599, Feb. 2020.
- [14] C. Hua, L. Zhang, and X. Guan, "Decentralized output feedback adaptive NN tracking control for time-delay stochastic nonlinear systems with prescribed performance," *IEEE Trans. Neural Netw. Learn. Syst.*, vol. 26, no. 11, pp. 2749–2759, Nov. 2015.
- [15] W. Si, D. Dong, and F. Yang, "Decentralized adaptive neural prescribed performance control for high-order stochastic switched nonlinear interconnected systems with unknown system dynamics," *ISA Trans.*, vol. 84, pp. 55–68, Jan. 2019.
- [16] Q. Zhou, H. Li, L. Wang, and R. Lu, "Prescribed performance observer-based adaptive fuzzy control for nonstrict-feedback stochastic nonlinear systems," *IEEE Trans. Syst., Man, Cybern., Syst.*, vol. 48, no. 10, pp. 1747–1758, Oct. 2018.
- [17] A. Polyakov, D. Efimov, and W. Perruquetti, "Finite-time and fixed-time stabilization: Implicit Lyapunov function approach," *Automatica*, vol. 51, pp. 332–340, Jan. 2015.
- [18] M. Cai, P. Shi, and J. Yu, "Adaptive neural finite-time control of non-strict feedback nonlinear systems with non-symmetrical dead-zone," *IEEE Trans. Neural Netw. Learn. Syst.*, vol. 35, no. 1, pp. 1409–1414, Jan. 2024.
- [19] Y. Yao, J. Tan, J. Wu, and X. Zhang, "Event-triggered fixed-time adaptive neural dynamic surface control for stochastic non-triangular structure nonlinear systems," *Inf. Sci.*, vol. 569, pp. 527–543, Aug. 2021.
- [20] Z. Cuan, D.-W. Ding, Y. Ren, and X.-J. Li, "Adaptive fixed-time control for state-constrained high-order uncertain nonlinear cyber-physical systems under malicious attacks," *IEEE Trans. Fuzzy Syst.*, vol. 31, no. 12, pp. 4285–4297, Dec. 2023.
- [21] Y. Yao, J. Tan, J. Wu, X. Zhang, and L. He, "Prescribed tracking error fixed-time control of stochastic nonlinear systems," *Chaos Solitons Fractals*, vol. 160, Jul. 2022, Art. no. 112288.
- [22] J. Wu, X. Chen, Q. Zhao, J. Li, and Z.-G. Wu, "Adaptive neural dynamic surface control with prespecified tracking accuracy of uncertain stochastic nonstrict-feedback systems," *IEEE Trans. Cybern.*, vol. 52, no. 5, pp. 3408–3421, May 2022.
- [23] J. D. Sánchez-Torres, E. N. Sanchez, and A. G. Loukianov, "Predefined-time stability of dynamical systems with sliding modes," in *Proc. Amer. Control Conf. (ACC)*, 2015, pp. 5842–5846.
- [24] Y. Song, Y. Wang, J. Holloway, and M. Krstic, "Time-varying feedback for regulation of normal-form nonlinear systems in prescribed finite time," *Automatica*, vol. 83, pp. 243–252, Sep. 2017.
- [25] W. Li and M. Krstic, "Prescribed-time output-feedback control of stochastic nonlinear systems," *IEEE Trans. Autom. Control*, vol. 68, no. 3, pp. 1431–1446, Mar. 2023.
- [26] A.-M. Zou, Y. Liu, Z.-G. Hou, and Z. Hu, "Practical predefined-time output-feedback consensus tracking control for multiagent systems," *IEEE Trans. Cybern.*, vol. 53, no. 8, pp. 5311–5322, Aug. 2023.
- [27] Y. Yao, Y. Kang, Y. Zhao, P. Li, and J. Tan, "A novel prescribed-time control approach of state-constrained high-order nonlinear systems," *IEEE Trans. Syst., Man, Cybern., Syst.*, vol. 54, no. 5, pp. 2941–2951, May 2024.
- [28] Y. Yao, Y. Kang, Y. Zhao, P. Li, and J. Tan, "Prescribed-time output feedback control for cyber-physical systems under output constraints and malicious attacks," *IEEE Trans. Cybern.*, vol. 54, no. 11, pp. 6518–6530, Nov. 2024.
- [29] S. Sui, C. L. P. Chen, and S. Tong, "Finite-time adaptive fuzzy prescribed performance control for high-order stochastic nonlinear systems," *IEEE Trans. Fuzzy Syst.*, vol. 30, no. 7, pp. 2227–2240, Jul. 2022.
- [30] B. Xin, S. Cheng, Q. Wang, J. Chen, and F. Deng, "Fixed-time prescribed performance consensus control for multiagent systems with nonaffine faults," *IEEE Trans. Fuzzy Syst.*, vol. 31, no. 10, pp. 3433–3446, Oct. 2023.
- [31] Z. Liang, Z. Wang, J. Zhao, P. K. Wong, Z. Yang, and Z. Ding, "Fixed-time and fault-tolerant path-following control for autonomous vehicles with unknown parameters subject to prescribed performance," *IEEE Trans. Syst., Man, Cybern., Syst.*, vol. 53, no. 4, pp. 2363–2373, Apr. 2023.
- [32] H. Duan, Y. Yuan, and Z. Zeng, "Distributed robust learning control for multiple unmanned surface vessels with fixed-time prescribed performance," *IEEE Trans. Syst., Man, Cybern., Syst.*, vol. 54, no. 2, pp. 787–799, Feb. 2024.
- [33] K. Zhao, Y. Song, T. Ma, and L. He, "Prescribed performance control of uncertain Euler-Lagrange systems subject to full-state constraints," *IEEE Trans. Neural Netw. Learn. Syst.*, vol. 29, no. 8, pp. 3478–3489, Aug. 2018.
- [34] Y. Liu, X. Liu, Y. Jing, X. Chen, and J. Qiu, "Direct adaptive preassigned finite-time control with time-delay and quantized input using neural network," *IEEE Trans. Neural Netw. Learn. Syst.*, vol. 31, no. 4, pp. 1222–1231, Apr. 2020.
- [35] K. Sun, R. Guo, and J. Qiu, "Fuzzy adaptive switching control for stochastic systems with finite-time prescribed performance," *IEEE Trans. Cybern.*, vol. 52, no. 9, pp. 9922–9930, Sep. 2022.
- [36] Y. Yao, J. Tan, J. Wu, and X. Zhang, "Event-triggered finite-time adaptive fuzzy tracking control for stochastic nontriangular structure nonlinear systems," *Int. J. Fuzzy Syst.*, vol. 23, pp. 2157–2169, Jun. 2021.
- [37] Z. Gao, Y. Zhang, and G. Guo, "Finite-time fault-tolerant prescribed performance control of connected vehicles with actuator saturation," *IEEE Trans. Veh. Technol.*, vol. 72, no. 2, pp. 1438–1448, Feb. 2023.

- [38] S. Sui, C. L. P. Chen, and S. Tong, "A novel full errors fixed-time control for constraint nonlinear systems," *IEEE Trans. Autom. Control*, vol. 68, no. 4, pp. 2568–2575, Apr. 2023.
- [39] Y. Zhu et al., "Event-based enhancing prescribed performance control for stochastic non-triangular structure nonlinear systems: A MTBFs-based approach," *Nonlinear Dyn.*, vol. 113, pp. 533–545, Sep. 2024, doi: [10.1007/s11071-024-10242-5](https://doi.org/10.1007/s11071-024-10242-5).
- [40] K. Zhao, F. Lewis, and L. Zhao, "Unifying performance specifications in tracking control of MIMO nonlinear systems with actuation faults," *Automatica*, vol. 155, Sep. 2023, Art. no. 111102.
- [41] L. Li, K. Zhao, Z. Zhang, and Y. Song, "Dual-channel event-triggered robust adaptive control of strict-feedback system with flexible prescribed performance," *IEEE Trans. Autom. Control*, vol. 69, no. 3, pp. 1752–1759, Mar. 2024.
- [42] Z. Li, Y. Wang, and Y. Song, "Asymptotic tracking control of SISO nonlinear systems with unknown time-varying coefficients: A global performance guaranteed solution," *IEEE Trans. Syst., Man, Cybern., Syst.*, vol. 54, no. 6, pp. 3717–3727, Jun. 2024.
- [43] L. Li, K. Zhao, Y. Song, and F. L. Lewis, "On the uniformness of full-state error prescribed performance for strict-feedback systems," *IEEE Trans. Syst., Man, Cybern., Syst.*, vol. 54, no. 5, pp. 3022–3031, May 2024.
- [44] G. Zong, Q. Xu, X. Zhao, S.-F. Su, and L. Song, "Output-feedback adaptive neural network control for uncertain nonsmooth nonlinear systems with input deadzone and saturation," *IEEE Trans. Cybern.*, vol. 53, no. 9, pp. 5957–5969, Sep. 2023.
- [45] Y.-F. Gao, X.-M. Sun, C. Wen, and W. Wang, "Adaptive tracking control for a class of stochastic uncertain nonlinear systems with input saturation," *IEEE Trans. Autom. Control*, vol. 62, no. 5, pp. 2498–2504, May 2017.
- [46] Y. Liu, X. Yao, and W. Zhao, "Distributed neural-based fault-tolerant control of multiple flexible manipulators with input saturations," *Automatica*, vol. 156, Oct. 2023, Art. no. 111202, doi: [10.1016/j.automatica.2023.111202](https://doi.org/10.1016/j.automatica.2023.111202).
- [47] Y. Yang, J. Tan, and D. Yue, "Prescribed performance tracking control of a class of uncertain pure-feedback nonlinear systems with input saturation," *IEEE Trans. Syst., Man, Cybern., Syst.*, vol. 50, no. 5, pp. 1733–1745, May 2020.
- [48] Y. Sun, J. Liu, Y. Gao, Z. Liu, and Y. Zhao, "Adaptive neural tracking control for manipulators with prescribed performance under input saturation," *IEEE/ASME Trans. Mechatronics*, vol. 28, no. 2, pp. 1037–1046, Apr. 2023.
- [49] H. Shen, X. Yu, H. Yan, J. H. Park, and J. Wang, "Robust fixed-time sliding mode attitude control for a 2-DOF helicopter subject to input saturation and prescribed performance," *IEEE Trans. Transport. Electric.*, early access, May 17, 2024, doi: [10.1109/TTE.2024.3402316](https://doi.org/10.1109/TTE.2024.3402316).
- [50] K. Yong, M. Chen, Y. Shi, and Q. Wu, "Flexible performance-based robust control for a class of nonlinear systems with input saturation," *Automatica*, vol. 122, Dec. 2020, Art. no. 109268.
- [51] Y. Yao, Y. Kang, Y. Zhao, P. Li, and J. Tan, "Flexible prescribed performance output feedback control for nonlinear systems with input saturation," *IEEE Trans. Fuzzy Syst.*, vol. 32, no. 11, pp. 6012–6022, Nov. 2024.
- [52] Y. Yao, Y. Kang, Y. Zhao, J. Tan, L. Gu, and G. Shi, "Sliding flexible prescribed performance control for input saturated nonlinear systems," *IEEE Trans. Fuzzy Syst.*, early access, Dec. 12, 2024, doi: [10.1109/TFUZZ.2024.3516132](https://doi.org/10.1109/TFUZZ.2024.3516132).
- [53] H. Xie, G. Zong, D. Yang, X. Zhao, and Y. Yi, "Flexible-fixed-time-performance-based adaptive asymptotic tracking control of switched nonlinear systems with input saturation," *IEEE Trans. Autom. Sci. Eng.*, vol. 21, no. 4, pp. 6371–6382, Oct. 2024, doi: [10.1109/TASE.2023.3324953](https://doi.org/10.1109/TASE.2023.3324953).
- [54] R. Ji, S. S. Ge, and D. Li, "Saturation-tolerant prescribed control for nonlinear systems with unknown control directions and external disturbances," *IEEE Trans. Cybern.*, vol. 54, no. 2, pp. 877–889, Feb. 2024.
- [55] R. Ji, B. Yang, J. Ma, and S. S. Ge, "Saturation-tolerant prescribed control for a class of MIMO nonlinear systems," *IEEE Trans. Cybern.*, vol. 52, no. 12, pp. 13012–13026, Dec. 2022.
- [56] K. Yong, M. Chen, W. Liu, and Q. Wu, "Flexible performance-based neural network control for mechanical systems under DoS attack and event triggering," *IEEE/ASME Trans. Mechatronics*, vol. 28, no. 4, pp. 2119–2130, Aug. 2023.
- [57] K. Yong, M. Chen, Y. Shi, and Q. Wu, "Flexible performance-based control for nonlinear systems under strong external disturbances," *IEEE Trans. Cybern.*, vol. 54, no. 2, pp. 762–775, Feb. 2024.
- [58] T. Shi, P. Shi, and J. Chambers, "Dynamic event-triggered model predictive control under channel fading and denial-of-service attacks," *IEEE Trans. Autom. Sci. Eng.*, vol. 21, no. 4, pp. 6448–6459, Oct. 2024, doi: [10.1109/TASE.2023.3325534](https://doi.org/10.1109/TASE.2023.3325534).
- [59] B. Yan, Y. Sun, P. Shi, and C.-C. Lim, "Event and learning-based resilient formation control for multiagent systems under DoS attacks," *IEEE Trans. Syst., Man, Cybern., Syst.*, vol. 54, no. 8, pp. 4876–4886, Aug. 2024, doi: [10.1109/TSMC.2024.3400879](https://doi.org/10.1109/TSMC.2024.3400879).